

Dopamine-Mo^{VI} complexation-assisted large-scale aqueous synthesis of single-layer MoS₂/carbon sandwich structure for ultrafast, long-life lithium-ion batteries

Chenyang Zhao,^a Junhua Kong,^a Liping Yang,^b Xiayin Yao,^a Si Lei Phua^a and Xuehong Lu^{*a}

^a School of Materials Science and Engineering, Nanyang Technological University, 50 Nanyang Avenue, 639798, Singapore.

^b Institute of Chemical and Engineering Sciences, A*STAR, 1 Pesek Road, Jurong Island, Singapore 627833, Singapore.

Experimental Section

Materials

Dopamine hydrochloride (DOPA-HCl), thioacetamide (TAA), sodium molybdate dihydrate (Na₂MoO₄·2H₂O), sodium tungstate dihydrate (Na₂WO₄·2H₂O), ferric chloride hexahydrate (FeCl₃·6H₂O) and bulk MoS₂ powder (< 2 μm) were purchased from Sigma-Aldrich (USA) and used as received. Electrolyte (1M LiPF₆ in a mixture of ethylene carbonate (EC) and dimethyl carbonate (DMC) at a 1:1 volume ratio) and lithium foil were purchased from Charlston Technologies Pte Ltd (Singapore).

Synthesis of SLMoS₂/C composite

The SLMoS₂/C composite was synthesized using hydrothermal method. Typically, 300 mg Na₂MoO₄, 900 mg DOPA-HCl and 900 mg TAA were dissolved in 20 ml deionized water, respectively, and then transferred to a 100 ml Teflon-lined autoclave. The suspension was kept at 200 °C for 16 hours. After cooling down, the black precipitates were collected by centrifugation and washed with DI water and ethanol for 3 times. The obtained sample was annealed at 700 °C for 3 hours in argon to eliminate the surface functional groups.

Synthesis of Fe₃O₄/C and WO₂/C composites

1 mmol $\text{Na}_2\text{WO}_4 \cdot 2\text{H}_2\text{O}$ and $\text{FeCl}_3 \cdot 6\text{H}_2\text{O}$ were dissolved in 60 ml deionized water and then mixed with 4 mmol DOPA-HCl, respectively. The suspensions were transferred to a 100 ml Teflon-lined autoclave and kept at 160 °C for 16 hours directly. The obtained samples were annealed at 400 °C for 3 hours in argon.

Characterization

The morphologies of the samples were studied using a field-emission scanning electron microscope (FESEM, JEOL JSM 7600) at an accelerating voltage of 5 kV and a transmission electron microscope (TEM, JEOL 2100) at 200 kV. X-ray photoelectron spectroscopy (XPS) measurements were conducted on a Kratos Analytical AXIS His spectrometer with a monochromatized Al Ka X-ray source (1486.6 eV photons). X-ray diffraction (XRD) patterns were recorded on a Bruker GADDS X-ray diffractometer. Fourier transform infrared spectroscopic (FTIR) measurements were performed using a Shimadzu FTIR IR Prestige-21 using KBr pellets. The compositions of the samples were determined by thermogravimetric analysis (TGA, TA Q500). All the samples were heated from room temperature to 600 °C in air. The UV absorption spectra were measured using a Shimadzu UV-3600 UV-vis-NIR spectrophotometer. Raman spectra were obtained by using WITec CRM200 confocal Raman microscopy system (WITec, Germany) with a laser wavelength of 532 nm.

Electrochemical measurements

The electrochemical performances were evaluated with a standard CR2032 coin cell. A Celgard® 2600 membrane is used as the separator. The working electrode was composed of 70 wt% composites, 20 wt% Super P carbon black, and 10 wt% polyvinylidene fluoride. The typical loading of the anode in the electrode was 2 to 3 mg. The electrochemical tests were performed on a NEWARE BTS-5V10mA battery tester. The cells were cycled between

0.005~3.0 V vs Li^+/Li . The specific capacity and current density were calculated based on the weight of the SLMoS_2/C composite. The cyclic voltammetry (CV) was studied on a PGSTAT302N Autolab electrochemical workstation with a voltage window of 0.005~3.0 V and a scan rate of 0.1 mV/s. The electrochemical impedance spectroscopy (EIS) was measured in the frequency range of 10^{-2} to 10^6 Hz with an AC voltage amplitude of 5 mV.

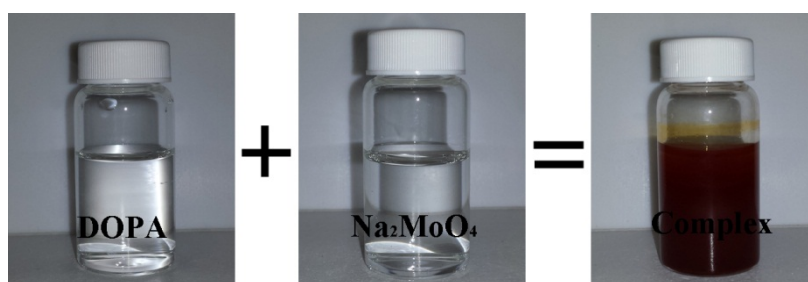


Fig. S1. Photo images of DOPA-HCl, Na_2MoO_4 and DMC solutions.

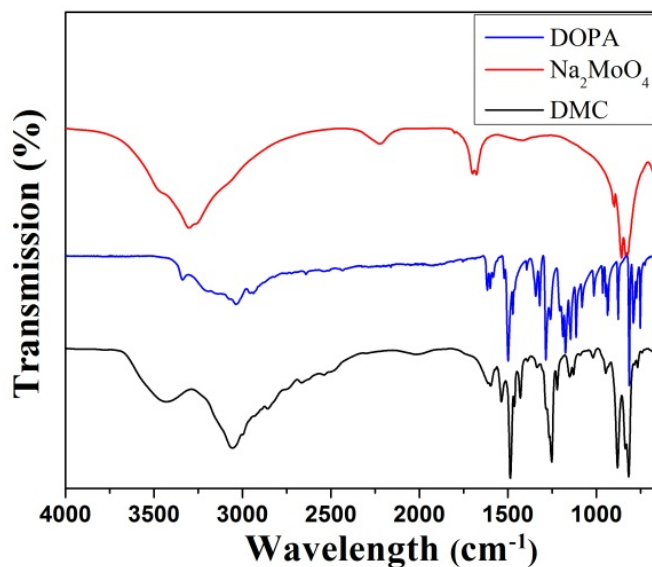


Fig. S2. FTIR spectra of DOPA-HCl, Na_2MoO_4 and DMC.

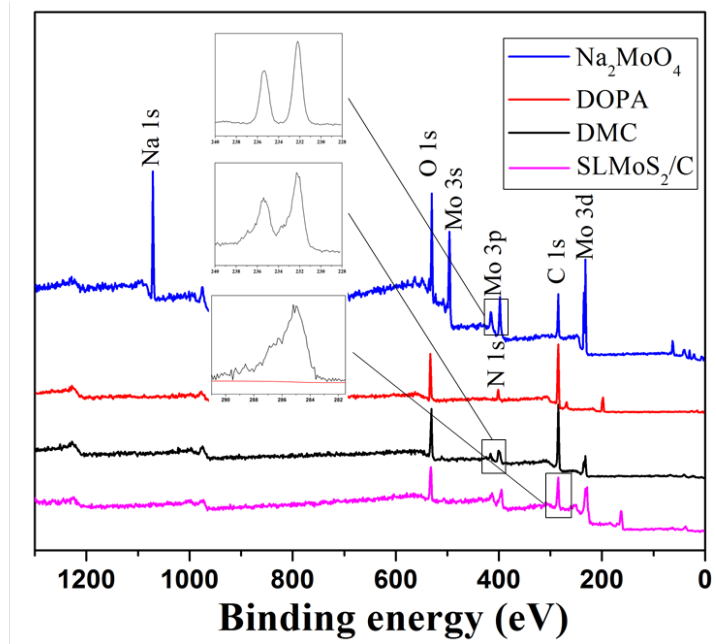


Fig. S3. XPS spectra of DOPA-HCl, Na_2MoO_4 , DMC and SLMoS_2/C .

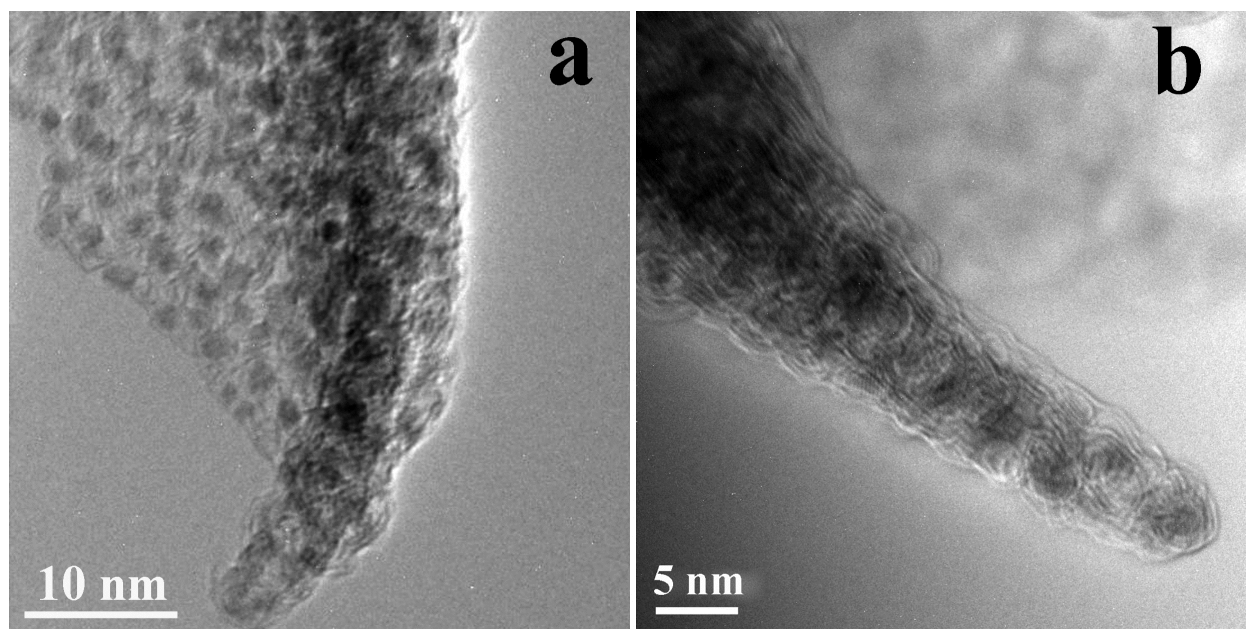


Fig. S4. TEM images of the DMC.

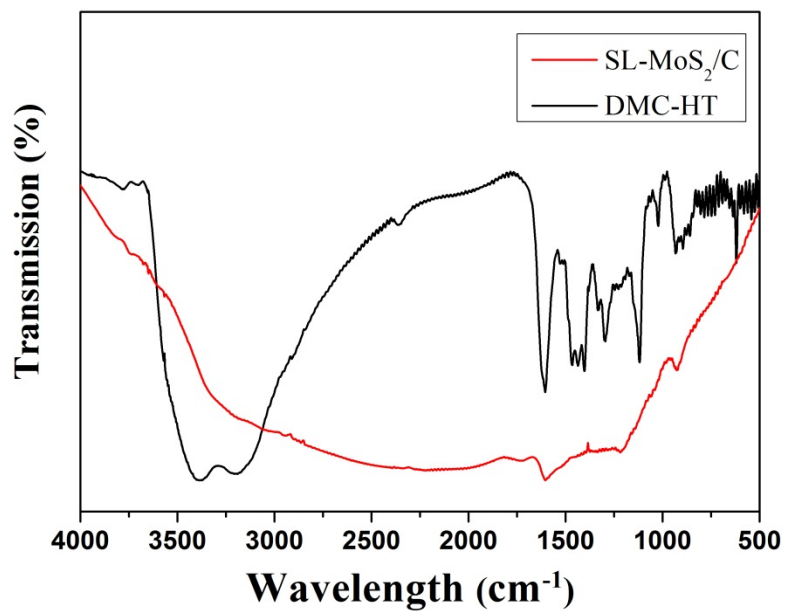


Fig. S5. FTIR spectra of the DMC-HT and SLMoS₂/C.

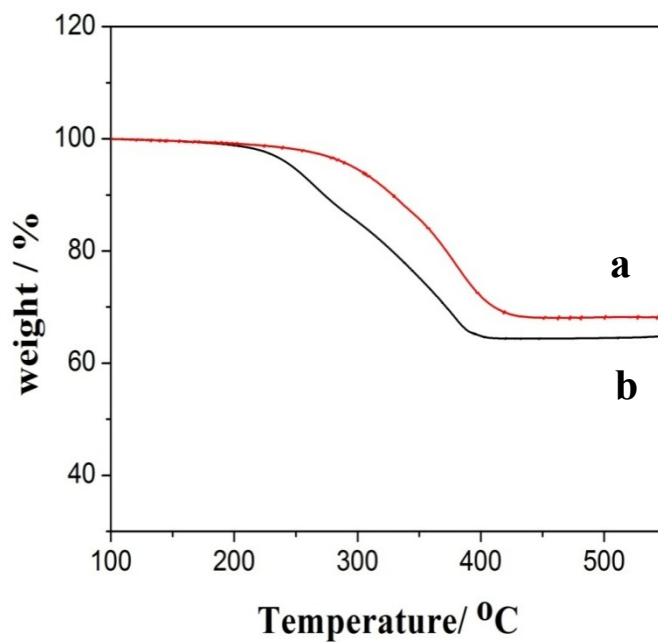


Fig. S6. TGA curves of (a) SLMoS₂/C and (b) DMC-HT. The large weight loss between 200-450 °C is caused by the combustion of carbon and conversion of MoS₂ to MoO₃ in air.

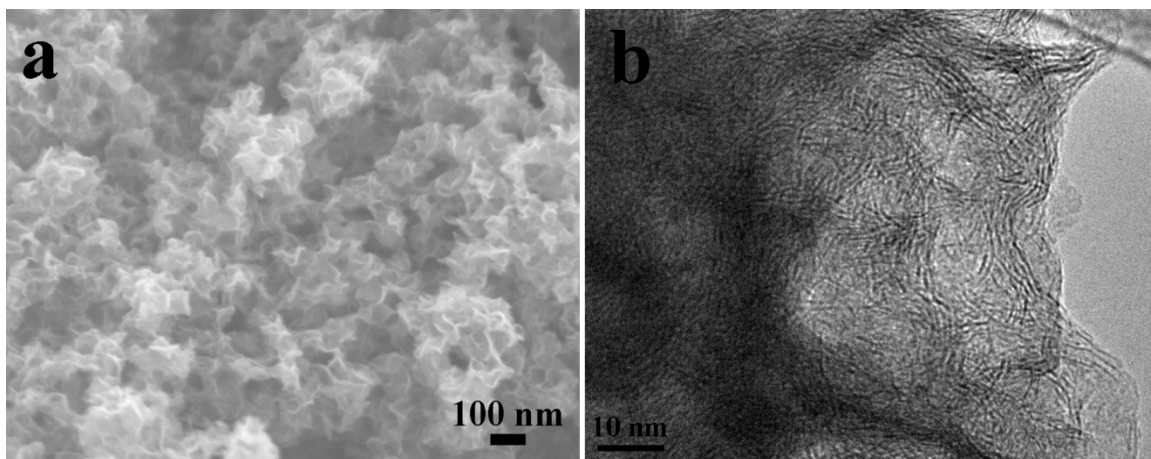


Fig. S7. (a) SEM and (b) TEM images of DMC-HT.

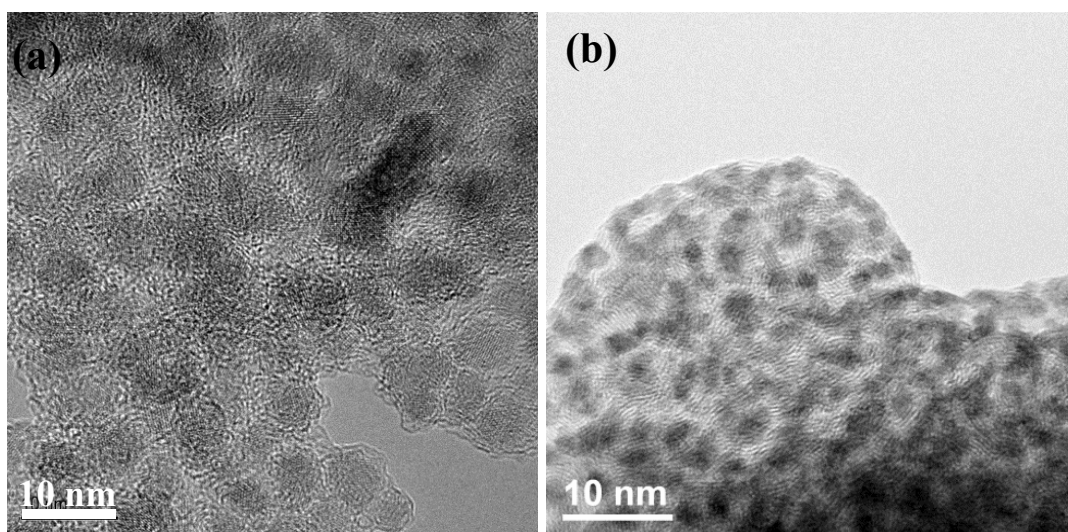


Fig. S8. TEM images of (a) Fe₃O₄/C and (b) WO₂/C composites after annealing.

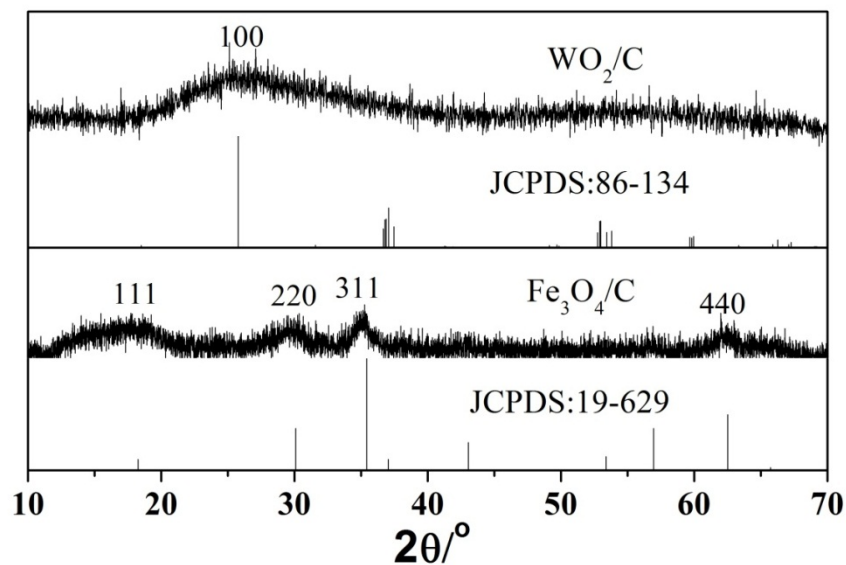


Fig. S9 XRD patterns of $\text{Fe}_3\text{O}_4/\text{C}$ and WO_2/C nanocomposites.

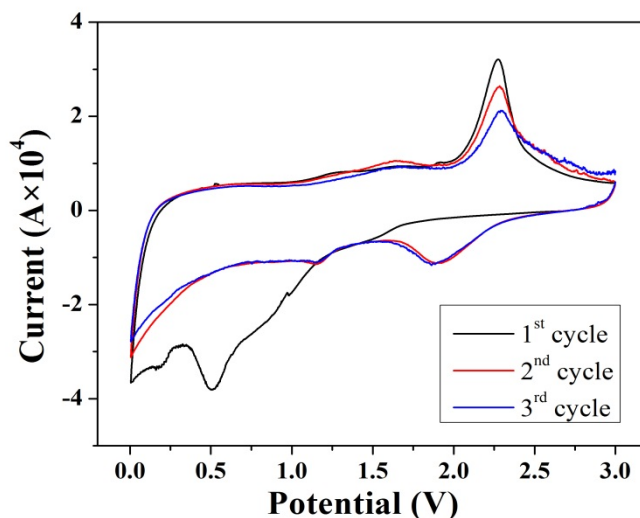


Fig. S10. Cyclic voltammogram of the SLMoS_2/C anode.

In the first discharge, a slope starts at about 1.5 V is indicative of the formation of Li_xMoS_2 . The inconspicuous conversion is caused by the expanded (002) spacing, low crystallinity and disordered structure of SLMoS_2 ¹⁻³. The Li_xMoS_2 then decomposes into Mo nanoparticles embedded in Li_2S matrix, giving a cathodic peak at about 0.5 V. The slope below 0.25 V is

assigned to the formation of a solid electrolyte interphase (SEI) film. During the anodic scanning, Li^+ stored within the carbon and defects of SLMoS_2/C are firstly released, together with the partially oxidation of Mo, leading to broad oxidation peaks centered at about 0.5 V and 1.3 V, respectively. The pronounced peak at about 2.3 V is associated with the oxidation of Li_2S to sulfur.⁴ Therefore, MoS_2 converts to a mixture of sulfur and Mo metal after the first cycle. Accordingly in the following cycles, the reduction peak at 2.0 V can be attributed to the formation of Li_2S , and the association of Li^+ ions with Mo is found at 1.0 V.⁵

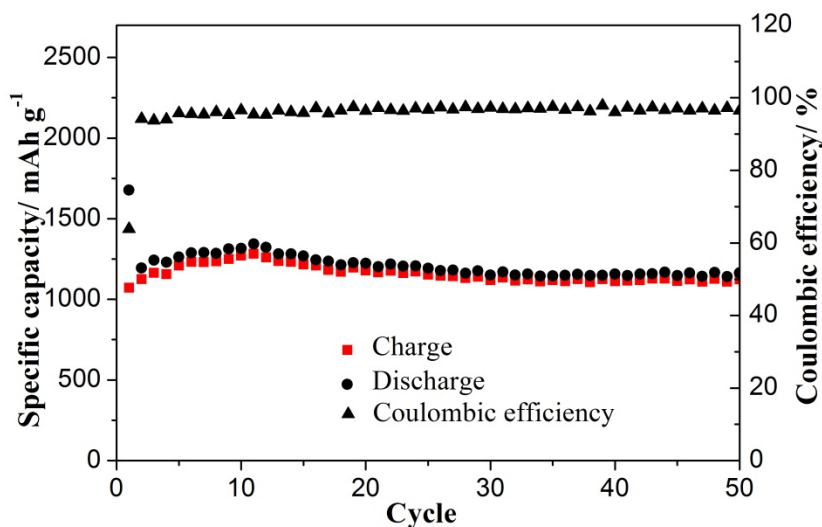


Fig. S11. Cycling performance of the SLMoS_2/C anode at a current density of 50 mA/g.

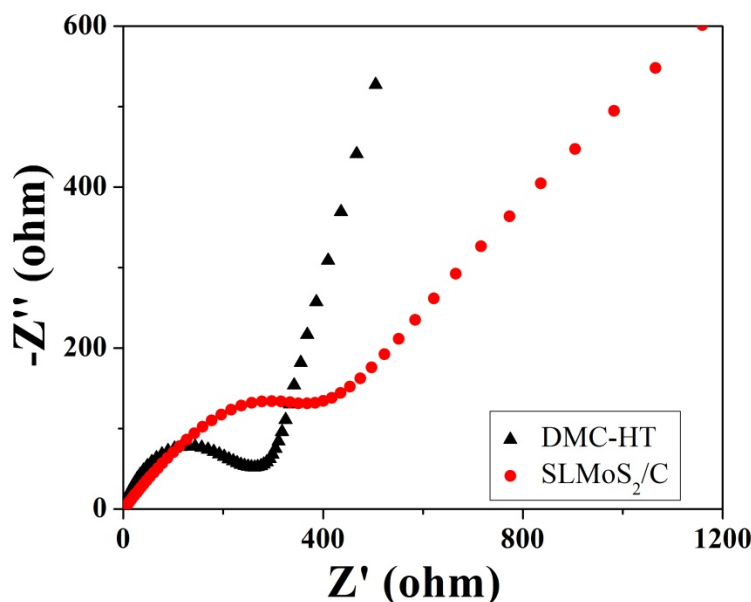


Fig. S12. Nyquist plot of SLMoS₂/C (a) before and (b) after cycles.

The Nyquist plots SLMoS₂/C anodes consist of one semicircle at high and medium frequencies and a straight line at low frequencies, corresponding to the charge transfer resistance at the electrolyte/electrode interface and the solid-state diffusion resistance of Li⁺ in the electrode, respectively. After cycling, the interfacial charge-transfer resistance increases because of the SEI layer formed and destruction of the MoS₂ structure during cycling.

references

1. K. Chang and W. Chen, *J. Mater. Chem.*, 2011, **21**, 17175.
2. Z. Wang, T. Chen, W. Chen, K. Chang, L. Ma, G. Huang, D. Chen and J. Y. Lee, *J. Mater. Chem. A*, 2013, **1**, 2202.
3. H. Hwang, H. Kim and J. Cho, *Nano Lett.*, 2011, **11**, 4826.
4. X. Fang, X. Yu, S. Liao, Y. Shi, Y.-S. Hu, Z. Wang, G. D. Stucky and L. Chen, *Microporous Mesoporous Mater.*, 2012, **151**, 418.
5. J. Xiao, X. Wang, X.-Q. Yang, S. Xun, G. Liu, P. K. Koech, J. Liu and J. P. Lemmon, *Adv. Funct. Mater.*, 2011, **21**, 2840.